

# Optimization of lag time underlies antibiotic tolerance in evolved bacterial populations

Ofer Fridman<sup>1</sup>, Amir Goldberg<sup>1</sup>, Irine Ronin<sup>1</sup>, Noam Shores<sup>2</sup> & Nathalie Q. Balaban<sup>1</sup>

The great therapeutic achievements of antibiotics have been dramatically undercut by the evolution of bacterial strategies that overcome antibiotic stress<sup>1,2</sup>. These strategies fall into two classes. ‘Resistance’ makes it possible for a microorganism to grow in the constant presence of the antibiotic, provided that the concentration of the antibiotic is not too high. ‘Tolerance’ allows a microorganism to survive antibiotic treatment, even at high antibiotic concentrations, as long as the duration of the treatment is limited. Although both resistance and tolerance are important reasons for the failure of antibiotic treatments<sup>3–6</sup>, the evolution of resistance<sup>7–9</sup> is much better understood than that of tolerance. Here we followed the evolution of bacterial populations under intermittent exposure to the high concentrations of antibiotics used in the clinic and characterized the evolved strains in terms of both resistance and tolerance. We found that all strains adapted by specific genetic mutations, which became fixed in the evolved populations. By monitoring the phenotypic changes at the population and single-cell levels, we found that the first adaptive change to antibiotic stress was the development of tolerance through a major adjustment in the single-cell lag-time distribution, without a change in resistance. Strikingly, we found that the lag time of bacteria before regrowth was optimized to match the duration of the antibiotic-exposure interval. Whole genome sequencing of the evolved strains and restoration of the wild-type alleles allowed us to identify target genes involved in this antibiotic-driven phenotype: ‘tolerance by lag’ (*tbl*). Better understanding of lag-time evolution as a key determinant of the survival of bacterial populations under high antibiotic concentrations could lead to new approaches to impeding the evolution of antibiotic resistance.

We exposed batch cultures of the bacterium *Escherichia coli* to a high concentration of ampicillin ( $100 \mu\text{g ml}^{-1}$ ), which is 15 times greater than the minimum inhibitory concentration (MIC), in a cyclic manner. The frequency of mutants that were resistant to this concentration<sup>10</sup> was less than  $10^{-11}$ . In each cycle (Fig. 1a), parallel overnight cultures in small volumes were resuspended in fresh medium containing ampicillin. After a fixed duration,  $T_a$ , of daily exposure to the antibiotic, the cultures were washed to remove the drug, resuspended in fresh medium and grown overnight. We evolved six populations, two for each of the three exposure durations:  $T_a = 3, 5$  and  $8 \text{ h}$ . In all cases, the bacteria soon adapted to the stressful regimen, and follow-up experiments established the genetic basis of this adaptation.

In the first cycle, the proportion of surviving bacteria at each  $T_a$  was less than 0.1%. After eight to ten cycles, ampicillin became at least an order of magnitude less effective at killing the bacteria (Fig. 1b and Extended Data Fig. 1). The increased survival rate of the evolved bacteria could have been achieved by a mutation that conferred resistance. We found, however, that the MIC of ampicillin for clones isolated from the evolved lines (*tbl3a*, *tbl5a* and *tbl8a*, evolved at  $T_a = 3, 5$  and  $8 \text{ h}$ , respectively) was indistinguishable from that for their ancestors (Fig. 1c). Similar to the MIC, the measure MDK<sub>99</sub> (the minimum duration for killing 99% of cells) may be defined to quantify tolerance (Box 1). A higher tolerance translates to a longer MDK<sub>99</sub>; that is, a treatment of longer duration

is needed to reach the same level of killing. We measured the MDK<sub>99</sub> for the wild-type and evolved strains and found that the MDK<sub>99</sub> of the evolved population increased with the duration of the stress period, reaching values as high as 15 times the MDK<sub>99</sub> of the wild-type strain (Fig. 1d). We conclude that these populations have all adapted to the antibiotic regimen through tolerance and not resistance.

Different mechanisms can enable bacteria to endure an interval of exposure to antibiotics. One way to achieve tolerance is by slowed growth<sup>11</sup>. However, no reduction in growth that could account for the observed tolerance was measured (Extended Data Fig. 2a). Another strategy for tolerance is related to the cells being in stationary phase before exposure to antibiotics, resulting in a delay in regrowth when switched to a new environment. By extending the time to first division (the single-cell

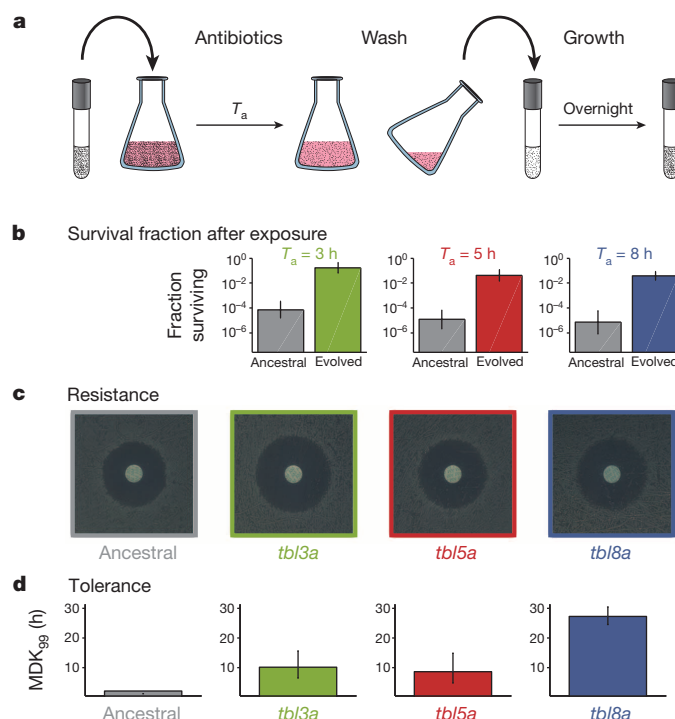


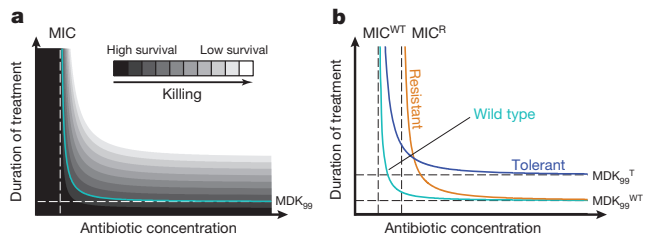
**Figure 1 | Resistance and tolerance of the evolved strains.** **a**, Experimental design for cyclic exposure to antibiotics. In each cycle, a small-volume overnight culture was resuspended in a larger volume of fresh medium containing  $100 \mu\text{g ml}^{-1}$  ampicillin for an exposure time  $T_a$ . After the antibiotic was washed out, the culture was resuspended in fresh medium and grown overnight. **b**, Survival of the evolved strains and ancestral strain after  $100 \mu\text{g ml}^{-1}$  ampicillin treatment for  $T_a = 3, 5$  or  $8 \text{ h}$ : strains *tbl3a*, *tbl5a* and *tbl8a*, respectively (see Extended Data Table 1). Data are presented as the mean  $\pm$  s.d. of two independent experiments. **c**, MIC test carried out using disc diffusion antibiotic sensitivity testing. **d**, Increase in tolerance of the evolved strains. MDK<sub>99</sub> (see Box 1) was determined by measuring the time to kill 99% of the population. Data are presented as the mean  $\pm$  s.d. from four experiments.

<sup>1</sup>Racah Institute of Physics, The Sudarsky Center for Computational Biology and the Center for NanoScience, Edmond J. Safra Campus, The Hebrew University, Jerusalem 91904, Israel. <sup>2</sup>Broad Institute of Harvard and MIT, Cambridge, Massachusetts 02142, USA.

## BOX 1

## Schematics of resistance and tolerance to bactericidal antibiotics

An antibiotic treatment is characterized by the concentration at which it is administered and its duration. The outcome of a treatment can be quantified by the fraction of bacteria killed by the drug. The curves (Box 1 Figure, panel a) indicate lines of equal killing for the wild-type (WT) strain. The cyan curve represents the combinations of treatment durations and concentrations that result in 99% killing. The curve displays two asymptotic behaviours: the vertical asymptote shows the concentration below which the culture will not be killed, even for a very long antibiotic treatment, namely the MIC. The horizontal asymptote shows the characteristic time needed to kill 99% of the culture, in the limit of high antibiotic concentrations. We term this asymptotic value the minimum duration for killing, or  $MDK_{99}$ . Schematics of the 99% killing curves for WT (cyan), resistant (R, orange) and tolerant (T, blue) strains are shown in Box 1 Figure, panel b. An increase in resistance translates into a shift in the MIC to higher concentrations, whereas an increase in tolerance manifests as a shift in the  $MDK_{99}$  to longer treatment durations.



lag time<sup>12</sup>) and remaining longer in a dormant state, a cell may avoid the harms of antibiotics. A case in point is the tolerance of type I persistent bacteria<sup>2</sup>, which is based on the existence of a subpopulation of cells with sufficiently long single-cell lag times<sup>13</sup>. To explore the possibility of the evolution of a lag-time-related strategy, we directly monitored, under the microscope, the time to first division of single cells taken from an overnight culture in stationary phase (Fig. 2a). Whereas cells from the ancestral clone divided within half an hour, the lag times of the evolved cells were distributed over many hours.

To corroborate that extended lag time is the main factor reducing the killing rate by ampicillin in our protocol, we measured the survival of evolved clones under exposure to norfloxacin, a drug that belongs to a different class of bactericidal antibiotic. The expectation was that the benefits of the slow exit from the dormant phase are generic and would carry over to a different drug that targets growing bacteria<sup>14,15</sup>. Indeed, a comparable increase in tolerance to norfloxacin was observed for the evolved clones, ruling out the possibility that a specific ampicillin-associated mechanism was responsible for the increase in tolerance (Extended Data Fig. 2b). Furthermore, the protective effect of the lag time was negated when the evolved clones were maintained in the exponential growth phase, a condition under which neither stationary phase nor the subsequent lag phase are reached (Fig. 2b). These results establish that in our cyclic protocol, the adaptive trait conferring tolerance to antibiotic treatments is the extended single-cell lag time. We term this adaptation 'tolerance by lag' (*tbl*), to distinguish it from tolerance that may be due to other factors.

To quantify the extension of single-cell lag times at the population level, we measured the distribution of these times with our recently developed ScanLag set-up<sup>16</sup>. Measuring the lag times of hundreds of cells in each case, we used this method to obtain single-cell lag-time distributions for the ancestral population and for clones isolated from the end populations evolved under the three cyclic regimens (Fig. 2c, Supplementary Video 1 and Extended Data Fig. 3). For each of the empirical distributions,

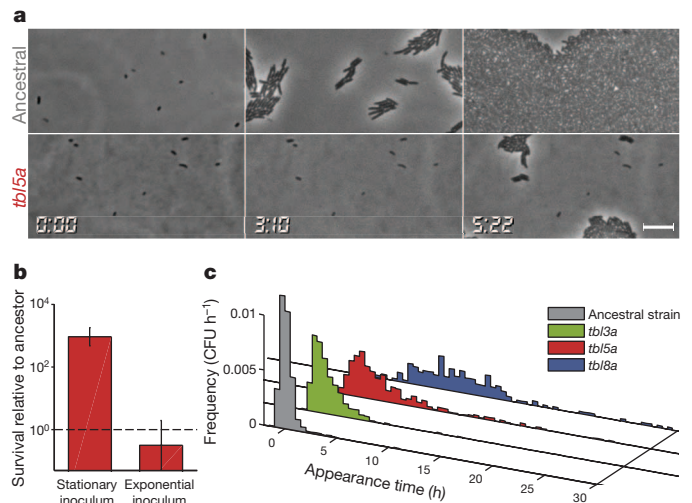


**Figure 2 | Changes in the single-cell lag-time distributions underlie antibiotic tolerance.** **a**, Phase-contrast images of time-lapse microscopy of single bacteria from a stationary culture plated on fresh medium show the extended lag of the evolved strain. Times are indicated in hours and minutes. Scale bar, 5  $\mu$ m. **b**, Survival advantage of the evolved strain (*tbl5a*) over the ancestral strain (shown as fold change) when exposed to ampicillin, after stationary phase or after exponential growth. The dashed line indicates ancestral survival. Data are presented as the mean  $\pm$  s.d. of three independent experiments. **c**, Measurement of the lag-time distribution with ScanLag. The appearance time of colonies was continuously monitored by an automated scanner system<sup>16</sup>. The histograms show the proportion of colony-forming units (CFUs) detected at each time point (mean = 0.78 h (ancestral), 2.1 h (*tbl3a*), 4.9 h (*tbl5a*), 10.3 h (*tbl8a*); median = 0.7 h (ancestral), 1.7 h (*tbl3a*), 3.7 h (*tbl5a*), 9.2 h (*tbl8a*), with s.e.m. below 8% and sample sizes of  $n = 514, 747, 423$  and 168, respectively). Colonies appearing at later times grow at the same rate (Extended Data Fig. 2a). Stationary cultures were grown from a single colony isolated from the majority clone of the end populations.

we calculated the mean single-cell lag time,  $\tau_{lag}$ . We found that  $\tau_{lag}$  increased from  $1.0 \pm 0.2$  h for the ancestral strain to several hours for the evolved strains. Specifically,  $\tau_{lag}$  was found to be  $3.4 \pm 1.0$  h,  $5.1 \pm 0.2$  h and  $10 \pm 1$  h for the clones that evolved in response to cyclic 3, 5 and 8 h exposures to antibiotic, respectively. These data show that the bacterial cultures under cyclic exposure to antibiotics adapted by extending the typical timescale of exit from the lag phase to approximately match the timescale of the antibiotic exposure.

While delaying the exit from lag phase provides protection from the antibiotic, a delay that is too long comes at the expense of time that could be spent proliferating once the antibiotics have been washed out. We explored this trade-off computationally, using a simple population-dynamics model that describes the growth and death of cells under cyclic antibiotic exposure (Fig. 3a–c and see Methods). By approximating the empirical single-cell lag-time distribution as exponential, the fitness of a population is a function of two parameters: the mean lag time,  $\tau_{lag}$ , and the antibiotic-exposure time,  $T_a$ . We used the model to calculate the value of  $\tau_{lag}$  that maximizes the fitness for a fixed  $T_a$ , and we found that the optimal lag time increases linearly with  $T_a$ , which is in good agreement with the empirical results (Fig. 3d).

We examined the genetic basis of the *tbl* phenotype by sequencing clones derived from the evolved populations (see Supplementary Methods)<sup>17</sup>. In each clone, few mutations were found, with a total of eight mutations across all sequenced clones being confirmed by Sanger sequencing. All mutations were in coding regions and were non-synonymous, suggesting that the affected proteins have a functional role in the *tbl* phenotype. To explore this possibility, we restored the wild-type alleles in the evolved strains and identified which genes restored the wild-type lag time; we defined these genes as *tbl* genes (Extended Data Fig. 4). Of the six genes affected by the eight mutations, three were found to be *tbl* genes by this definition (Extended Data Tables 1 and 2). Notably, we observed

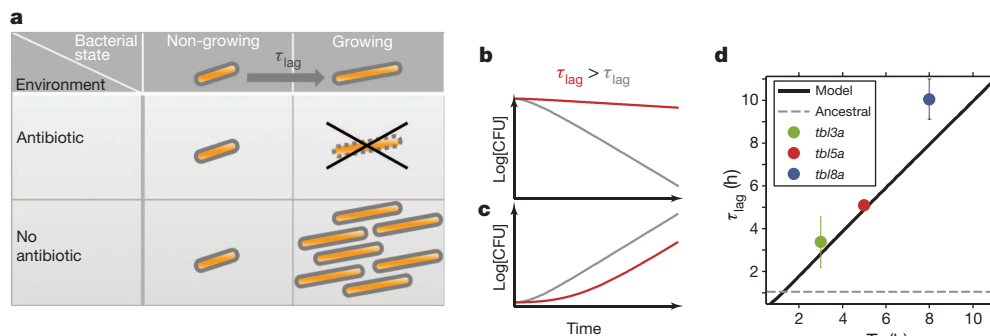


**Figure 3 | Optimization of lag time.** **a**, Schematic illustration of the processes in the theoretical model for the optimization of lag time. The fate of bacteria is determined by their growth state and by the environment. The non-growing phase (lag) protects the bacteria from the antibiotics. **b**, **c**, Non-growing bacteria switch to the growing state with a typical timescale of  $\tau_{\text{lag}}$ . The trade-off of extending the lag time is illustrated by two strains: one with a short  $\tau_{\text{lag}}$  (grey), and the other with a long  $\tau_{\text{lag}}$  (red). In the presence of antibiotics, the longer  $\tau_{\text{lag}}$

reduces the killing and increases tolerance (**b**). In the absence of antibiotics, the longer  $\tau_{\text{lag}}$  delays the resumption of growth and bears a fitness cost (**c**). **d**, Lag time as a function of duration of antibiotic treatment,  $T_a$ . The empirical mean lag-time dependence (circles) of the evolved *tbl* clones follows the model predictions for lag-time optimization (solid line). Data are presented as the mean  $\pm$  s.d. of three independent experiments. The dashed line is the mean lag time of the ancestral strain.

different mutations within the same gene in different clones, indicating that these genes are under strong selection. All *tbl* genes were found to have fixed mutations in the evolved populations (Extended Data Table 3).

The *tbl* gene candidates are associated with several pathways. Two of these pathways, toxin–antitoxin modules<sup>18,19</sup> and aminoacyl-transfer RNA synthetase<sup>20–22</sup>, have been implicated in increased persistence. Interestingly, quantitative analysis has shown that toxin–antitoxin modules are a network motif that is ideally suited to set the timescale of the single-cell lag-time distribution<sup>23</sup>. In contrast to these pathways, no relationship between the third emerging pathway, *prs*, and either lag or tolerance has been described in the literature. More experiments are needed to understand the relationship between the essential *prs* gene and the *tbl* phenotype.

The evolution of the lag-time distribution is a remarkable demonstration of an adaptation not to the specific nature of an environmental stress but to its duration. Not only does this finding illustrate that temporal parameters associated with growth can be readily changed during evolution<sup>24</sup>, but also the correspondence between stress duration and the timescale of the evolved phenotypes shows how fine-tuned this adaptation can be. It is also notable that the malleable trait here is the lag time. Lag is commonly viewed as an inevitable delay in adjustment to new conditions imposed by metabolic constraints. Our study shows this phenotype in a different light: extended lag time as an advantageous trait for avoiding growth in adverse conditions and a trait that can evolve to accommodate selective pressures.

In fact, it is the entire distribution of single-cell lag times that sets the fitness of the population, and it is the distribution as a whole that is being shaped during evolution. In a short period, the populations in this study adapted to antibiotic pressure by extending the single-cell lag-time distribution (Fig. 2c). While the shift in the mean lag time is beneficial, this is not the case for the corresponding increase in variance. Indeed, for our regimen, maximum fitness is reached if all cells exit lag together, at the end of the antibiotic-exposure period. The observed increase in both the mean and the variance of the lag-time distribution is interesting and may indicate that those parameters are constrained at the molecular level to evolve concomitantly. Such an increase in variance could itself reflect past selection for a bet-hedging strategy<sup>25,26</sup>, as variance in the single-cell lag times does make sense when the duration of the antibiotic-exposure interval is not completely predictable. More generally, the time-scales and stochasticity of the environmental sequence of conditions<sup>27</sup> may shape the single-cell lag-time distribution beyond changes in the mean and variance<sup>26</sup>, as in the case of type I persistence to antibiotic treatments, in which only a fraction of the population is tolerant through having a long lag time<sup>13</sup>. It should be noted that in our evolved strains, the whole population becomes tolerant (Extended Data Fig. 1).

From a clinical point of view, tolerance by lag presents a major challenge<sup>28</sup>: in contrast to the specificity of resistance, the *tbl* phenotype confers a survival advantage against a broad spectrum of drugs and stresses. The revised understanding of antimicrobial tolerance offered here suggests new ways to eliminate bacterial populations, such as interfering with the precursor signal (stationary phase) from which bacteria anticipate stress. In addition, it is possible that tolerance facilitates the subsequent evolution of antibiotic resistance and that reducing tolerance might impede the emergence of antibiotic resistance. Understanding tolerance, resistance and the interplay between them in the adaptation of microorganisms to drugs is a critical goal in addressing the decreased efficacy of antibiotics<sup>29</sup>.

## METHODS SUMMARY

**Evolutionary protocol of cyclic exposure to antibiotics.** Evolution under cyclic antibiotic exposure consisted of three steps. First, an overnight culture (0.5 ml;  $1 \times 10^9$  bacteria) was resuspended in 50 ml LB broth Lennox (LBL) supplemented with  $100 \mu\text{g ml}^{-1}$  ampicillin (Sigma) and incubated at  $37^\circ\text{C}$  with shaking at 300 r.p.m. for  $T_a$  hours ( $T_a = 3, 5$  or  $8$  h). Second, the antibiotic-containing medium was removed by washing twice in LBL (10 min centrifugation at  $1,400g$ ). Last, the culture was resuspended in 1 ml fresh LBL and grown overnight (for approximately 20, 18 and 15 h, for the  $T_a = 3, 5$  and  $8$  h cultures, respectively) at  $37^\circ\text{C}$  with shaking. It should be noted that nearly all of the surviving cells were kept from cycle to cycle, thus minimizing drift; this is in contrast to typical serial dilution evolution experiments, in which most of the culture is discarded<sup>30</sup>.

**Single-cell lag-time distribution measurement with ScanLag.** Overnight cultures grown from a single colony were plated at appropriate dilutions on solid LBL agar medium supplemented with  $12.5 \mu\text{g ml}^{-1}$  chloramphenicol (Sigma). A custom, automated scanner array set-up was used to monitor the appearance of thousands of colonies on plates over several days and to extract lag-time distributions by automated image analysis<sup>16</sup>. Single-cell microscopic observations confirmed that the delay in colony appearance was due to an extended lag.

**Theoretical model.** The model describes a bacterial population consisting of two phenotypes, lagging (*L*) and growing (*G*) bacteria, whose dynamics are governed by first-order, linear differential equations:  $\dot{G} = \alpha(G/\tau_{\text{grow}}) + (L/\tau_{\text{lag}})$  and  $\dot{L} = -(L/\tau_{\text{lag}})$ , where  $1/\tau_{\text{lag}}$  is the rate at which lagging bacteria switch to growth and  $1/\tau_{\text{grow}}$  is the growth rate. The outcome depends on the environment and is captured by the parameter  $\alpha$ : in the absence of antibiotics, division leads to population growth and  $\alpha = 1$ ; however, when antibiotics are present, the cells that try to divide die, and  $\alpha = -1$ .

**Online Content** Methods, along with any additional Extended Data display items and Source Data, are available in the online version of the paper; references unique to these sections appear only in the online paper.

Received 1 November 2013; accepted 12 May 2014.

Published online 25 June 2014.

1. Bush, K. *et al.* Tackling antibiotic resistance. *Nature Rev. Microbiol.* **9**, 894–896 (2011).



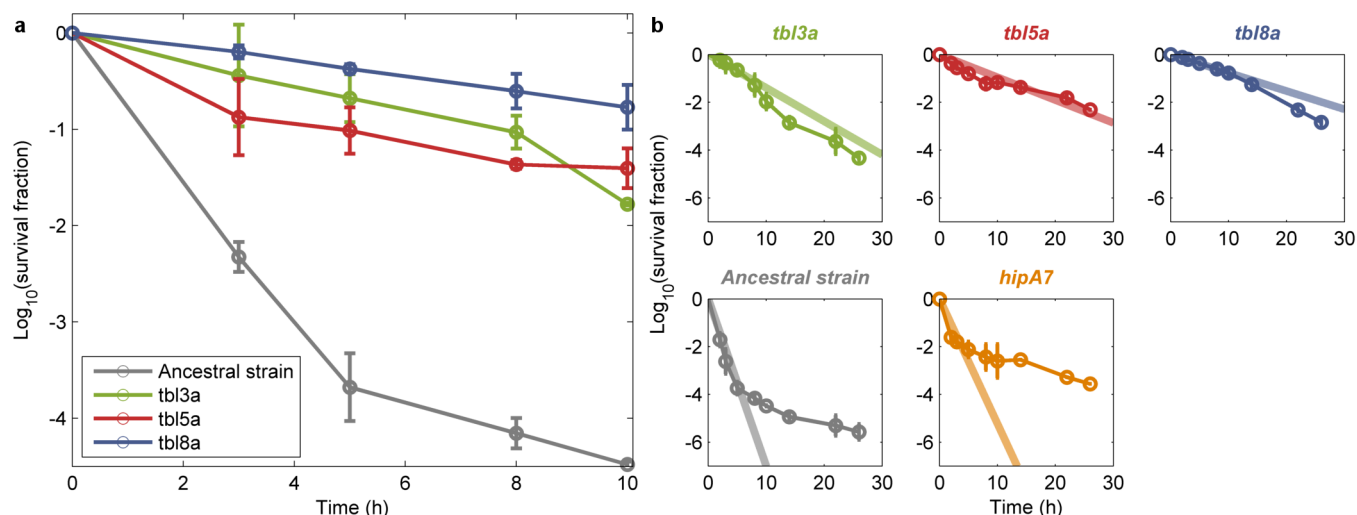
2. Balaban, N., Merrin, J., Chait, R., Kowalik, L. & Leibler, S. Bacterial persistence as a phenotypic switch. *Science* **305**, 1622–1625 (2004).
3. Collignon, P. Antibiotic resistance. *Med. J. Aust.* **177**, 325–329 (2002).
4. Spellberg, B., Powers, J., Brass, E., Miller, L. & Edwards, J. Trends in antimicrobial drug development: implications for the future. *Clin. Infect. Dis.* **38**, 1279–1286 (2004).
5. Fauvar, M., De Groote, V. & Michiels, J. Role of persister cells in chronic infections: clinical relevance and perspectives on anti-persister therapies. *J. Med. Microbiol.* **60**, 699–709 (2011).
6. Lewis, K. Persister cells. *Annu. Rev. Microbiol.* **64**, 357–372 (2010).
7. Toprak, E. *et al.* Evolutionary paths to antibiotic resistance under dynamically sustained drug selection. *Nature Genet.* **44**, 101–105 (2012).
8. Gullberg, E. *et al.* Selection of resistant bacteria at very low antibiotic concentrations. *PLoS Pathogens* **7** (2011).
9. Lee, H., Molla, M., Cantor, C. & Collins, J. Bacterial charity work leads to population-wide resistance. *Nature* **467**, 82–85 (2010).
10. Olsson, O., Bergström, S., Lindberg, F. & Normark, S. *ampC*  $\beta$ -lactamase hyperproduction in *Escherichia coli*: natural ampicillin resistance generated by horizontal chromosomal DNA transfer from *Shigella*. *Proc. Natl Acad. Sci. USA* **80**, 7556–7560 (1983).
11. Gilbert, P., Collier, P. & Brown, M. Influence of growth rate on susceptibility to antimicrobial agents: biofilms, cell cycle, dormancy, and stringent response. *Antimicrob. Agents Chemother.* **34**, 1865–1868 (1990).
12. Baranyi, J. Stochastic modelling of bacterial lag phase. *Int. J. Food Microbiol.* **73**, 203–206 (2002).
13. Gefen, O. & Balaban, N. The importance of being persistent: heterogeneity of bacterial populations under antibiotic stress. *FEMS Microbiol. Rev.* **33**, 704–717 (2009).
14. Tuomanen, E., Cozens, R., Tosch, W., Zak, O. & Tomasz, A. The rate of killing of *Escherichia coli* by  $\beta$ -lactam antibiotics is strictly proportional to the rate of bacterial growth. *J. Gen. Microbiol.* **132**, 1297–1304 (1986).
15. Wolfson, J., Hooper, D., McHugh, G., Bozza, M. & Swartz, M. Mutants of *Escherichia coli* K-12 exhibiting reduced killing by both quinolone and  $\beta$ -lactam antimicrobial agents. *Antimicrob. Agents Chemother.* **34**, 1938–1943 (1990).
16. Levin-Reisman, I. *et al.* Automated imaging with ScanLag reveals previously undetectable bacterial growth phenotypes. *Nature Methods* **7**, 737–739 (2010).
17. Goecks, J., Nekrutenko, A., Taylor, J. & Galaxy, T. Galaxy: a comprehensive approach for supporting accessible, reproducible, and transparent computational research in the life sciences. *Genome Biol.* **11**, R86 (2010).
18. Black, D., Kelly, A., Mardis, M. & Moyed, H. Structure and organization of *hip*, an operon that affects lethality due to inhibition of peptidoglycan or DNA synthesis. *J. Bacteriol.* **173**, 5732–5739 (1991).
19. Gerdes, K. & Maisonneuve, E. Bacterial persistence and toxin–antitoxin loci. *Annu. Rev. Microbiol.* **66**, 103–123 (2012).
20. Girgis, H., Harris, K. & Tavazoie, S. Large mutational target size for rapid emergence of bacterial persistence. *Proc. Natl Acad. Sci. USA* **109**, 12740–12745 (2012).
21. Kaspy, I. *et al.* HipA-mediated antibiotic persistence via phosphorylation of the glutamyl-tRNA-synthetase. *Nature Commun.* **4**, 3001 (2013).
22. Germain, E., Castro-Roa, D., Zenkin, N. & Gerdes, K. Molecular mechanism of bacterial persistence by HipA. *Mol. Cell* **52**, 248–254 (2013).
23. Rotem, E. *et al.* Regulation of phenotypic variability by a threshold-based mechanism underlies bacterial persistence. *Proc. Natl Acad. Sci. USA* **107**, 12541–12546 (2010).
24. Oxman, E., Alon, U. & Dekel, E. Defined order of evolutionary adaptations: experimental evidence. *Evolution* **62**, 1547–1554 (2008).
25. Beaumont, H., Gallie, J., Kost, C., Ferguson, G. & Rainey, P. Experimental evolution of bet hedging. *Nature* **462**, 90–93 (2009).
26. Kussell, E., Kishony, R., Balaban, N. & Leibler, S. Bacterial persistence: a model of survival in changing environments. *Genetics* **169**, 1807–1814 (2005).
27. Mitchell, A. *et al.* Adaptive prediction of environmental changes by microorganisms. *Nature* **460**, 220–224 (2009).
28. Nahata, M., Vashi, V., Swanson, R., Messig, M. & Chung, M. Pharmacokinetics of ampicillin and sulbactam in pediatric patients. *Antimicrob. Agents Chemother.* **43**, 1225–1229 (1999).
29. Cohen, N., Lobritz, M. & Collins, J. Microbial persistence and the road to drug resistance. *Cell Host Microbe* **13**, 632–642 (2013).
30. Barrick, J. *et al.* Genome evolution and adaptation in a long-term experiment with *Escherichia coli*. *Nature* **461**, 1243–1247 (2009).

**Supplementary Information** is available in the online version of the paper.

**Acknowledgements** We thank I. Levin-Reisman for discussions and technical help with the ScanLag system, S. Belkin for strains, and the National BioResource Project and National Institute of Genetics, Japan, for the Keio collection deletion mutants. The work was supported by the European Research Council (Starting Grant no. 260871) and the Israel Science Foundation (no. 592/10). O.F. acknowledges support from the Levzion Fellowship.

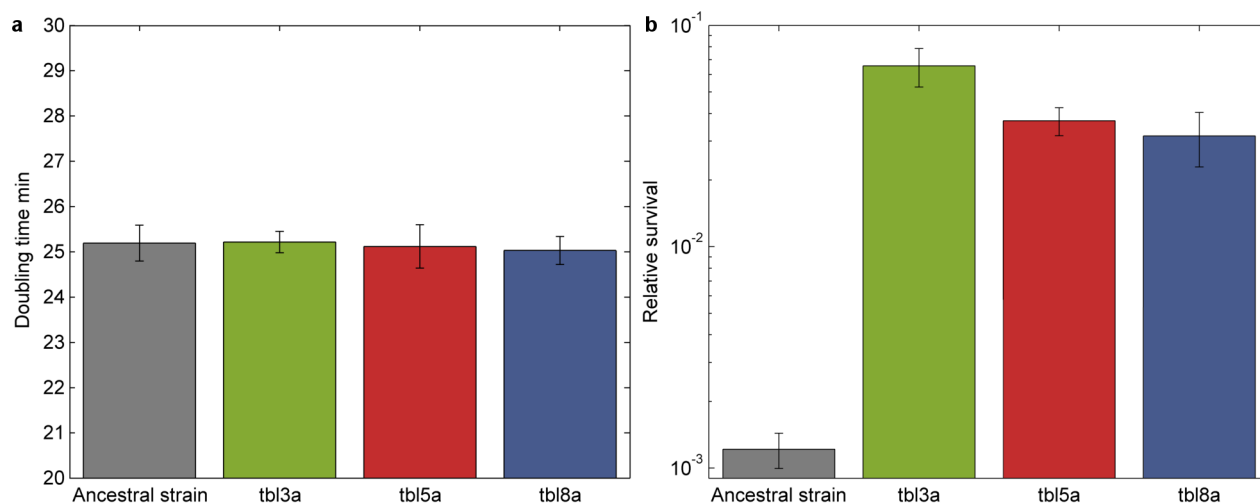
**Author Contributions** N.Q.B. and O.F. designed the experiments. O.F. performed the experiments. O.F. and N.Q.B. analysed the data. O.F. and N.S. performed the theoretical analysis. O.F. and A.G. analysed the whole genome sequencing data. I.R. made the genetic reconstructions. N.Q.B. and N.S. wrote the manuscript.

**Author Information** Whole genome sequence data of KLY (ancestral), *tbl3a* *tbl5a* and *tbl8a*, as well as reconstructed ancestral genome sequence data, have been deposited in the BioProject database under the accession number PRJNA229104. Reprints and permissions information is available at [www.nature.com/reprints](http://www.nature.com/reprints). The authors declare no competing financial interests. Readers are welcome to comment on the online version of the paper. Correspondence and requests for materials should be addressed to N.Q.B. ([nathalieqb@phys.huji.ac.il](mailto:nathalieqb@phys.huji.ac.il)).



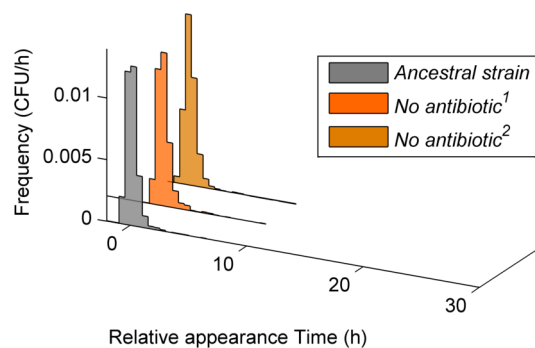
**Extended Data Figure 1 | Killing curves of the evolved clones indicate tolerance to ampicillin treatment.** **a**, Cultures were grown overnight from a single colony for each evolved *tbl* clone. The survival of the cultures was determined as previously described<sup>2</sup>. Data are presented as the mean  $\pm$  s.d. of two independent experiments. **b**, Determining whether the evolved strains show a persistent phenotype: a sub-population of persisters is characterized by a significant slowing of the killing rate compared with the rate at which the bulk of the bacterial population (99%) is dying from the treatment, as indicated by the straight line on each graph. The point (on the y axis) at which an upward

departure from this line occurs indicates the size of that subpopulation. The *hipA7* strain (orange) shows such a slowing corresponding to  $10^{-2}$ – $10^{-1}$  of the cells being persistent. The wild-type ancestral strain (grey) also exhibits this behaviour but at a persister population that is at least two orders of magnitude smaller. None of the evolved strains shows a marked decrease in the killing rate at frequencies comparable to or larger than the ancestral persistence level. Therefore, the increased survival of the evolved strains is characterized as tolerance.

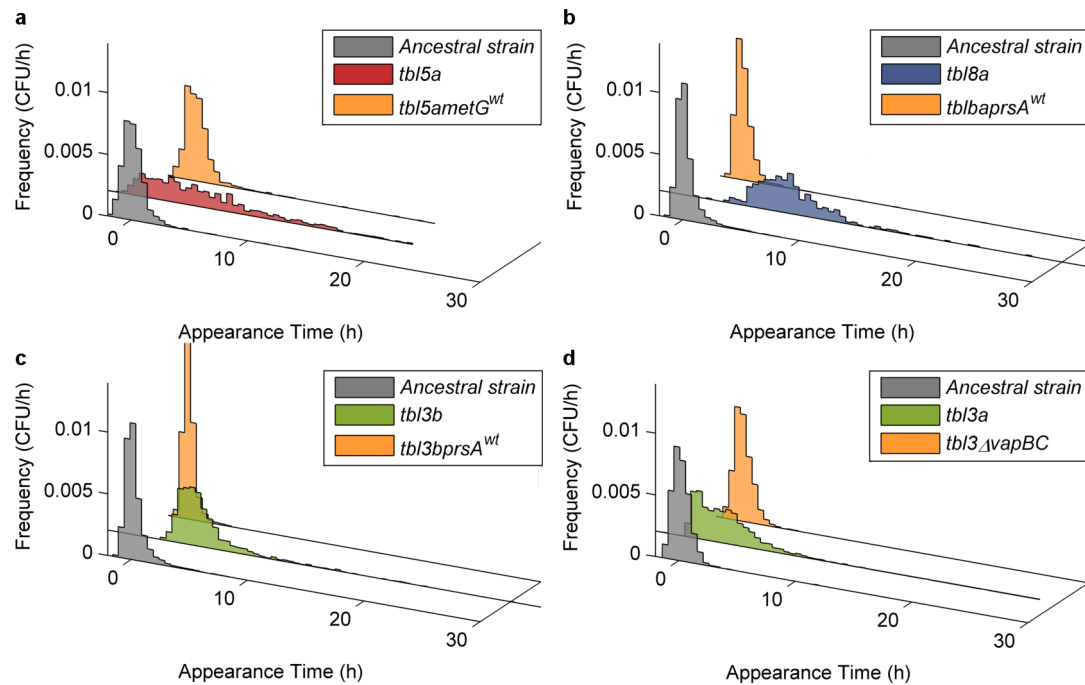


**Extended Data Figure 2 | Extended phenotypic analysis of the ancestral strain and the clones evolved under cyclic antibiotic exposure.** **a**, The growth rates of evolved clones show no significant difference from the ancestral strain. The cultures of each clone were grown in a 24-well plate and the optical density at 630 nm ( $OD_{630}$ ) was measured over time. The doubling times were

extracted from the fit to the exponential growth phase. Data are presented as the mean  $\pm$  s.d. of four replicates. **b**, Survival rates after 10 h under  $8 \mu\text{g ml}^{-1}$  norfloxacin treatment of the ancestral strain and the evolved clones. Data are presented as the mean  $\pm$  s.d. of two independent experiments.



**Extended Data Figure 3 | Evolution under the same protocol without antibiotic exposure shows no lag extension.** Two parallel bacterial lines ('No antibiotic', orange shades) were subjected to the same protocol as the cyclic antibiotic exposure but without antibiotics. Instead, the cultures were diluted 1:100 in fresh medium without ampicillin. The colony appearance time was continuously monitored by ScanLag, an automated scanner system<sup>16</sup>. The histograms show the fraction of CFUs detected at each time point for the ancestral strain (grey), line one (dark orange) and line two (light orange) ( $n = 1,080, 1,320$  and  $1,833$ , respectively).



**Extended Data Figure 4 | Restoration of *tbl* gene wild-type alleles restores the ancestral single-cell lag-time distribution.** Colony appearance time was continuously monitored by ScanLag, an automated scanner system<sup>16</sup>. The histograms show the fraction of CFUs detected at each time point: ancestral strain (grey), *tbl5a* (red), *tbl5a* with restored *metG* (orange) ( $n = 1,409$ , 1,099 and 1,029, respectively; temperature ( $T$ ) = 32 °C) (a); ancestral strain (grey), *tbl8a* (blue), *tbl8a* with restored *prsa* (orange) ( $n = 2,245$ , 1,288 and 2,285,

respectively) (b); ancestral strain (grey), *tbl3b* (green), *tbl3b* with restored *prsa* (orange) ( $n = 2,245$ , 441 and 1,936, respectively) (c); and ancestral strain (grey), *tbl3a* (green), *tbl3a* with deletion of toxin-antitoxin *vapBC* ( $n = 1,140$ , 1,571 and 902, respectively;  $T = 32$  °C) (d). All evolved bacterial clones form colonies at later times, whereas restoration of the wild-type alleles, or deletion of the mutated module, abolishes the long lag.



**Extended Data Table 1 | *tbl* genes identified by whole genome sequencing of evolved strains**

Strain	T <sub>a</sub> (Hours)	Genomic position	Mutation	Amino Acid Substitution	Annotation	Clone isolated in cycle #
<i>tbl5a</i>	5	2171860	T>A	Y620N	<i>metG</i> (methionyl-tRNA synthetase)	10
<i>tbl5b</i>	5	3049094 - 3049117	inversion		<i>vapB</i> antitoxin homolog(*) 24bp inversion, flanked by 8bp IRs	10
<i>tbl3a</i>	3	3049134	A>T	V5E	<i>vapB</i> antitoxin homolog(*)	8
<i>tbl3b</i>	3	1245467	C>T	R79H	<i>prs</i> (ribose-phosphate diphosphokinase)	8
<i>tbl8a</i>	8	1245524	C>T	C60Y	<i>prs</i> (ribose-phosphate diphosphokinase)	8

\* Note that despite 100% similarity with *vapB*, in several annotations a different open reading frame (*trbH*) is identified on the complementary strand.

Extended Data Table 2 | Additional mutations identified by whole genome sequencing of evolved strains

Strain	T <sub>a</sub> (Hours)	Genomic position	Mutation	Amino Acid Substitution	Annotation	Clone isolated in cycle #
<i>tbl5a</i>	5	3454381	T>G	D19A	<i>sspA</i> (stringent starvation protein A)	10
<i>tbl5b</i>	5	714095	T>G	W503G	<i>pgm</i> (phosphoglucomutase)	10
<i>tbl5b</i>	5	1846085	Insertion Element <i>insB</i>		<i>yeal</i> (predicted diguanylate cyclase)	

**Extended Data Table 3 | Evaluation of fixation frequencies of the *tbI* genes**

Mutated gene	Fixated strain	Cycle of fixation	Frequency *
<i>metG</i> (methionyl-tRNA synthetase)	<i>tbI5a</i>	10	100%
<i>vapB</i> antitoxin homolog	<i>tbI3a</i>	8	89±5%
<i>prs</i> (ribose-phosphate diphosphokinase)	<i>tbI8a</i>	10	100%

Three *tbI* genes (*metG*, *vapB* and *prsA*) were identified by whole genome sequencing of one clone from each evolved line. Mutations were identified in each of the sequenced clones. Analysis led to the identification of the few mutations that led to the *tbI* phenotype in those clones (see Supplementary Methods). To determine whether those mutations had fixed in their respective populations (that is, represent the majority of the culture's evolution), we randomly isolated a total of 46 colonies from three different lines directly from the frozen batch cultures. We sequenced the *tbI* genes of those colonies by Sanger sequencing and found the *tbI* mutations had fixed in all of the lines. In two lines, the fixation was found in 100% of the clones; in one line, 17 out of 19 colonies had the *tbI* mutations, and 2 colonies had the wild-type allele.

\* Calculated from the Sanger sequencing results of *N* colonies isolated directly from the evolved batch cultures (*n* = 11 (*tbI5a*), 19 (*tbI3a*) and 16 (*tbI8a*)).